Supporting Information: *cis* to *trans* isomerization of azobenzene derivatives studied with transition path sampling and QM/MM molecular dynamics

Anja Muzdalo,[†] Peter Saalfrank,[‡] Jocelyne Vreede,[¶] and Mark Santer[*,†]

†*Department of Theory and Biosystem, Max Planck Institute of Colloids and Interfaces, 14424 Potsdam, Germany*

‡*Department of Chemistry, University of Potsdam, 14476 Potsdam, Germany*

¶*Computational Chemistry, Van't Hoff Institute for Molecular Sciences, University of Amsterdam, 1098 XH Amsterdam, The Netherlands*

E-mail: mark.santer@mpikg.mpg.de

Phone: +49 (0)331 5679610. Fax: +49 (0)331 5679602

1 Structural parameters of AB and pp-AB from DFT/DFTB methods

In Table 1 Structural parameters for AB and pp-AB from structure optimizations in vacuum are displayed for *cis* and *trans* isomers. Note the different signs appearing for PBE and DFTB3 in the listing for AB(*trans*), these represent the same structure as found for B3LYP and DFTBA; the difference between DFTBA and DFTB3 for pp-AB (*cis*), on the other hand, is related to the convergence towards a second minimum very close in energy. For

DFTBA, for example, the second minimum is at $\phi' = 59°$ and $\phi = 39°$.

Table 1: Structural parameters of AB and pp-AB in selected DFT/DFTB models from structural optimization in the gas phase. $r_{N'N}$ and r_{NC} denote the central N′=N bond length and that between N (the inversion center) and C1. The basis set for DFT calculations was 6-31G*. All angles are given in degrees.

Parameter	ω	α	α'	ϕ	ϕ'	r_{NC}[Å]	$r_{N'N}$[Å]
AB(*cis*)							
B3LYP	9.78	124.12	124.12	50.09	49.88	1.4357	1.2495
PBE	11.99	123.98	123.98	47.42	47.37	1.4343	1.262
DFTBA	10.67	120.49	120.50	51.63	51.63	1.4203	1.2681
DFTB3	9.99	121.41	121.35	54.21	54.15	1.4397	1.2637
AB(*trans*)							
B3LYP	180.00	114.81	114.81	0.01	0.01	1.4186	1.2606
PBE	-180.00	114.16	114.16	-0.02	0.02	1.4184	1.2767
DFTBA	180.00	113.86	113.86	0.02	0.00	1.4128	1.2860
DFTB3	-179.96	114.56	114.56	0.17	0.64	1.4304	1.2935
pp-AB(*cis*)							
B3LYP	12.50	126.14	124.79	32.34	57.60	1.4138	1.2545
PBE	16.03	125.97	125.18	27.74	54.36	1.4087	1.2683
DFTBA	-14.16	122.12	120.89	-37.95	-54.16	1.4086	1.2730
DFTB3	14.13	123.71	121.39	39.74	58.12	1.4218	1.2678
pp-AB(*trans*)							
B3LYP	-178.17	114.83	115.99	5.88	7.04	1.3956	1.2683
PBE	-176.85	114.24	115.55	6.88	10.12	1.3926	1.2862
DFTBA	-177.04	114.62	113.70	5.19	15.48	1.4058	1.2927
DFTB3	-176.20	114.15	115.47	4.20	22.17	1.4815	1.3019

2 Methods extended

Steered MD

Steered MD is simply regular (stochastic) MD with a superimposed restraining harmonic potential on a set of selected coordinates $\vec{X}$. That is, to the system Hamiltonian a potential term of the form

$$V(\vec{X}, t) = 0.5\kappa(t) \left(\vec{X} - \vec{X}_0(t) \right)^2 \tag{1}$$

is added with time-dependent minimum at $\vec{X}_0$. This allows to "drag" the coordinates by a certain amount in a specified time. To find an initial steered transition path we had $X_0(t)$ vary from $X = 0.84$ (*cis*) to $X = -0.84$ (*trans*) within 500 (vacuum) or 1000 (MM solvent) time steps with $\kappa(t) = 1000$kJ/mole. To harvest the first unbiased reactive pathway we randomly picked a configuration during the time $X(t)$ passes the interface region I_{shoot}(e. g., close to the barrier top of $F(X)$) and restarted the dynamics by two-way shooting with momentum reversal. This process is repeated until a reactive pathway is generated and usually requires only a few attempts.

Metadynamics/biased dynamics

Metadynamics is distinguished from steered MD in that a biasing potential is build up over time, leading to a self-guided exploration of the free energy landscape in a set of selected collective coordinates $\vec{s}$. The biasing potential is history dependent and is written as

$$V(\vec{s},t) = \sum_{k\tau<t} W(k\tau) \exp\left(-\sum_{i=1}^{d} \frac{(s_i - s_i(q(k\tau)))^2}{2\sigma_i^2}\right) , \tag{2}$$

where the stride interval was $\tau = 0.5ps$, the height of the Gaussian potential $W(k\tau) = 2.0$kJ/mole for both collective variables ω and α, and the widths $\sigma_\omega = 11.5^\circ$ and $\sigma_\alpha = 5.7^\circ$, respectively. To achieve a well-tempered biasing, the Gaussian height was decreased with simulation time through the temperature parameter $\Delta T = 6.0$K,

$$W(k\tau) = W_0 \exp\left(-\frac{V(\vec{s}(q(k\tau)), k\tau)}{k_{\text{B}}\Delta T}\right), \tag{3}$$

$\vec{s} = (\omega, \alpha)$. This version of the metadynamics free energy method has been invented by Barducci, Bussi and Parrinello.[1]

As the metadynamics goes on, the bias potential lifts the system out of deeper energy wells and finally flattens the free energy landscape in the selected coordinates. Thus, the

potential build up is actually the negative of the free energy landscape.

Umbrella Sampling

Umbrella sampling in X has been carried out with restraining potentials of the form

$$V(X, X_i) = \frac{1}{2}\kappa(X - X_i)^2\,, \tag{4}$$

where $\kappa = 1100$kJ/mole for AB and $\kappa = 900$kJ/mole for pp-AB, and $X_{i+1} - X_i = 0.06$. In Figure 1 we show as an example the resulting ensemble of overlapping distributions in X for pp-AB in vacuum, ranging from $X_1 = -0.9$ to $X_{30} = +0.84$. Each restraint simulation was run for 5ns.

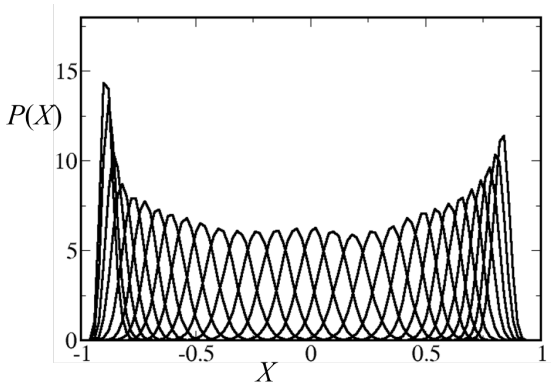

Figure 1: Normalized umbrella distributions in X for pp-AB in vacuum according to Equation 4. The increasing height of the distribution as the X_i approach ± 1 implies a reduction in width, indicating the limits in the range of definition for X.

3 Phenyl ring orientation

From figure 6 of the main text it was shown that during the TPS run, the relative orientation ϕ_{OR} varies little along single pathways. Figure 2 illustrates the residual amount of dynamics in ϕ_{OR} with the last accepted trajectories of each path ensemble, by aligning 20 molecular configurations equidistant in time with respect to the primed phenyl ring. The latter was

chosen because the phenyl torsion ϕ' virtually does not vary with the central torsion ω around the N′=N double bond, whereas the torsions around N′=N and N-C_1 (at the inversion center) show an almost linear dependence, compare Figure 3.

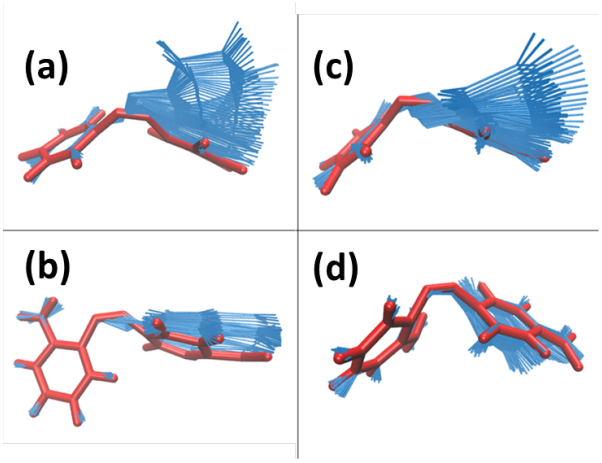

Figure 2: Cluster representations of the last accepted trajectories of the TPS ensembles in Figure 3 (a)-(d). Red liquorices: initial *cis* conformation; the overlaid structures (blue sticks) are aligned with respect to carbon atoms of the primed phenyl ring and the N′ atom in the sequence C1′-N′=N-C1 representing ω.

Superficially this is reminiscent of the "hula-twist" mechanism that is believed to play an important role especially in excited-state isomerization of azobenzene.[2] However, in all cases (a)-(d) there is at least some inversion component contained in the isomerization mechanism, and the significance of the twist mechanism is diminished.

In Figure 4 (upper panel) we show the distribution (PMF profiles) of the relative phenyl ring orientation ϕ_{OR} for AB and pp-AB in vacuum, for restraint simulations at $X = X^*$ with the bias potential Eq. 4 ($\kappa = 1000$kJ/mole). The lower panel shows the corresponding trajectories $\phi_{\mathrm{OR}}(t)$; even for the (relatively) short time of 400ps there is sufficient dynamics for the PMF curves to represent useful estimates. Note that the restraint in X does not impact ϕ, ϕ' or ϕ_{OR}. The $F(\phi_{\mathrm{OR}})$ are in full agreement with TPS results shown in Figure 6 of the main text: a rather broad minimum for AB, but with a preference for $\phi_{\mathrm{OR}} = 180°$; and a clear minimum at $\phi_{\mathrm{OR}} = 90°$ for pp-AB. For completeness, we show in Figure 5 $F(\phi_{\mathrm{OR}})$ for the corresponding *cis*- and *trans* states.

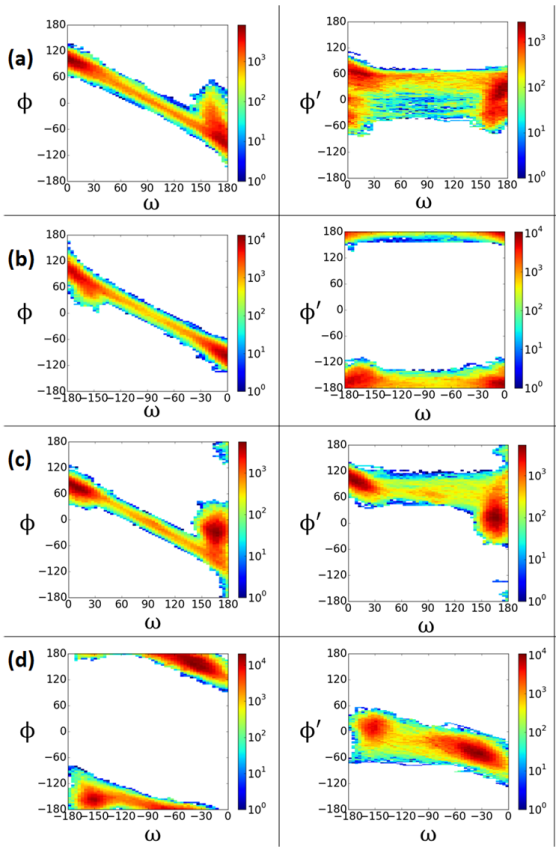

Figure 3: Projection of the TPS ensembles of (a) AB in vacuum, (b) pp-AB in vacuum, (c) AB in DMSO and (d) pp-AB in DMSO onto the variable pairs (ϕ, ω) and (ϕ', ω), in the left and right column, respectively.

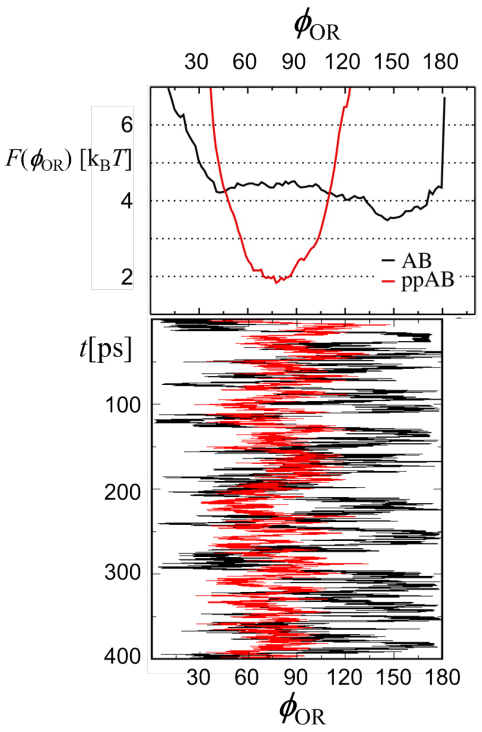

Figure 4: PMF maps in ϕ_{OR} acquired from 400ps long MD simulations in vacuum restrained at $X = X^*$. The lower panel shows the trajectories from which the $F(\phi_{OR})$ were generated by Boltzmann inversion. Here, time is in vertical direction, the horizontal axis is aligned (shared) with the ϕ_{OR} axis of the PMF graphs.

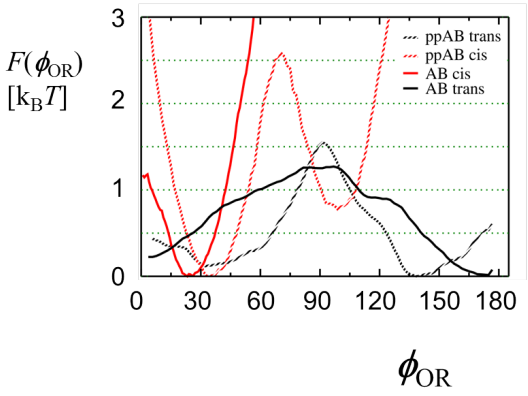

Figure 5: PMF maps in ϕ_{OR} acquired from 400ps long MD simulations analogous to Figure 4 in vacuum for AB and pp-AB in their *cis*- and *trans*-states at 333K (no restraints applied).

4 Molecular Mechanics parameters for toluene and DMSO

In Table 2 the LJ parameters are summarized that have been used for the QM/MM model of AB and pp-AB and the solvent. They have been taken from the General Amber Force Field (GAFF).[3] The partial charges for DMSO and toluene have been determined according to the standard 2-stage Amber protocol[4] with due symmetrization of chemically equivalent atoms. The charge density distribution has been determined at the HF/6-31G* level of theory. The final charges were calculated with a standalone version of the RESP program[5] and are reported in Figure 6.

Table 2: LJ parameters for DMSO and toluene, as well as for AB and pp-AB in the QM/MM setting, taken from the GAFF force field.

DMSO		
Atomtype	σ[nm]	ϵ[kJ/mole]
C	0.340	0.458
H	0.247	0.0657
S	0.356	1.046
O	0.296	0.879
Toluene		
Atomtype	σ[nm]	ϵ[kJ/mole]
CA	0.340	0.360
HA	0.260	0.0628
C	0.340	0.458
H	0.265	0.0657
pp-AB		
Atomtype	σ[nm]	ϵ[kJ/mole]
N, NH, NO	0.325	0.711
HA	0.260	0.0628
HN	0.107	0.0657
CA	0.340	0.360
O	0.296	0.879
AB		
Atomtype	σ[nm]	ϵ[kJ/mole]
N	0.325	0.711
CA	0.340	0.360
HA	0.260	0.0628

DMSO

S	0.26972
O	-0.54168
C	-0.24118
C1	-0.24118
H	0.12572
H1	0.12572
H2	0.12572
H3	0.12572
H4	0.12572
H5	0.12572

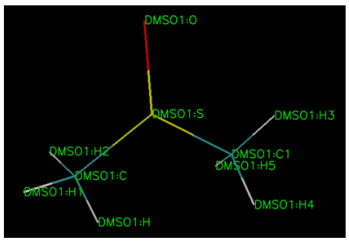

Toluene

C	-0.3839250
H	0.1062830
H1	0.1062830
C1	0.2875090
H2	0.1062830
C2	-0.2785960
C3	-0.1057810
C4	-0.1788650
C5	-0.1057810
C6	-0.2785960
H3	0.1569580
H4	0.1356710
H5	0.1399280
H6	0.1356710
H7	0.1569580

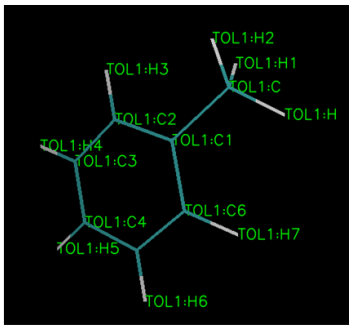

Figure 6: Partial charges for toluene and DMSO reported in units of the elementary charge $e = 1.602 \cdot 10^{-19}$C.

References

(1) Barducci, A.; Bussi, G.; Parrinello, M. Well-Tempered Metadynamics: A Smoothly Converging and Tunable Free Energy Method. *Phys. Rev. Lett.* **2008**, *100*, 020603–.

(2) Quick, M.; Dobryakov, A. L.; Gerecke, M.; Richter, C.; Berndt, F.; Ioffe, I. N.; Granovsky, A.; Mahrwald, R.; Ernsting, N.; Kovalenko, S. A. Photoisomerization Dynamics and Pathways of trans- and cis- Azobenzene in Solution from Broadband Femtosecond Spectroscopies and Calculations. *J. Phys. Chem. B* **2014**, *118*, 8756–8771.

(3) Wang, J.; Wolf, R. M.; Caldwell, J. W.; Kollman, P. A.; Case, D. A. Development and Testing of a General Amber Force Field. *J. Comp. Chem.* **2004**, *25*, 1157–1174.

(4) Bayly, C. I.; Cieplak, P.; Cornell, W. D.; Kollman, P. A. A Well-Behaved Electrostatic

Potential Based Method Using Charge Restraints for Deriving Atomic Charges: The RESP Model. *J. Phys. Chem.* **1993**, *97*, 10269–10280.

(5) Becker, J. P.; Wang, F.; Cieplak, P.; Dupradeau, F. Y. http://q4md-forcefieldtools.org.